Process Biochemistry 126 (2023) 216–222

Contents lists available at ScienceDirect

Process Biochemistry

journal homepage: www.elsevier.com/locate/procbio

Expression of a full-length influenza virus hemagglutinin in *Escherichia coli*

Yoonjin Bae [1], Jihwan Chun [1], Wonbeom Park [1], Seungjoo Kim, Soomin Kim, Nayeon Kim, Minju Kim, Seokoh Moon, Jaehyeon Hwang, Younghoon Jung, Dae-Hyuk Kweon [*]

Department of Integrative Biotechnology, College of Biotechnology and Bioengineering, Sungkyunkwan University, Suwon 16419, South Korea

ARTICLE INFO

Keywords:
Expression Engineering
Oct1-DBD
Caveolin 1
Influenza virus
Hemagglutinin

ABSTRACT

Fusion or co-expression with other proteins is an effective option for improving recombinant protein expression in prokaryotic hosts. In this study, recombinant *Escherichia coli* strains expressing full-length influenza hemagglutinin (HA) were constructed to test the effect of co-expression of Cav1 protein or fusion with Oct1 upon expression of soluble HA. While HA alone was not expressed, a large amount of HA expression was observed upon co-expression with Cav1, which forms heterologous caveolae in the cytosol. When the DNA-binding protein Oct1 was used as a fusion partner, the HA solubility was improved. This study demonstrates a novel approach to achieve soluble expression of HA in *E. coli*.

1. Introduction

The expression of hydrophobic recombinant proteins has been a major hurdle in protein engineering research, especially due to frequent formation of inclusion bodies [1]. Upon expression, recombinant proteins may encounter an exotic environment where pH, osmolarity, cofactors, folding mechanisms, and many other aspects differ from their native state. Consequently, newly synthesized polypeptides may fail to stabilize and can begin to aggregate instead [2]. Several experimental approaches are available for improving recombinant protein expression in *Escherichia coli* hosts, including but not limited to employing various vectors and host strains, slowing down production rate, supplementing with cofactors, fusion with a partner protein, and employing chemical or biological chaperones [1,3]. Otherwise, computational approaches can also be taken to facilitate experimental optimizations [4].

In this study, we employed chaperones and fusion partners to improve the solubility of influenza hemagglutinin (HA) (Fig. 1A) in *E. coli*. The lack of glycosidic moieties and the high hydrophobicity of HA render it extremely challenging to express. There are two major barriers to prokaryotic expression of influenza HA. First, the lack of an intracellular membrane structure in *E. coli* makes it difficult to express full-length HA, which includes a transmembrane domain [5,6]. Second, the hydrophobic moieties of HA are highly likely to misfold, leading to inclusion body formation or HA degradation [7,8]. As a countermeasure, we employed heterologous caveolin-1 (Cav1) as a chaperone (Fig. 1B) [5,9] and the Oct1 DNA-binding domain (Oct1 DBD) as a fusion partner (Fig. 1C) [10,11] and assessed the HA expression with or without them. Cav1 is a building block of cytoplasmic vesicles called heterologous caveolae (h-caveolae), and its co-expression has been shown to contribute to the expression of transmembrane SNARE (soluble N-ethylmaleimide-sensitive factor attachment protein receptor) in *E. coli* [5,9]. Oct1 DBD is one of the two functional domains of eukaryotic transcription activators, and as its name implies, it mediates binding of activator to target DNA [12]. In our previous publication, we confirmed that fusion with Oct1 DBD allows the fusion protein to form plasmid-protein complexes in *E. coli* cytoplasm, known as plasmid display, and facilitate the expression of recombinant protein in soluble form [10]. In this study, we could confirm the soluble expression of full-length HA, and we anticipate that our approach could contribute to efficient production of HA and hopefully other challenging recombinant proteins in *E. coli* [13–15].

2. Materials and methods

2.1. Strains and plasmids

All strains and plasmids used in this study are listed in Table 1. Plasmids (pHA2DFPDT, pHA2DFP, pHA, pOct1-HA, pMBP-Cav1, and pOct1-Cav1) were constructed as shown in Figs. 2–4. All cloning experiments were performed using a sequence- and ligation-independent

* Corresponding author.
E-mail address: dhkweon@skku.edu (D.-H. Kweon).
[1] These authors contributed equally to this work and share first authorship.

https://doi.org/10.1016/j.procbio.2023.01.008
Received 7 September 2022; Received in revised form 20 December 2022; Accepted 6 January 2023
Available online 9 January 2023

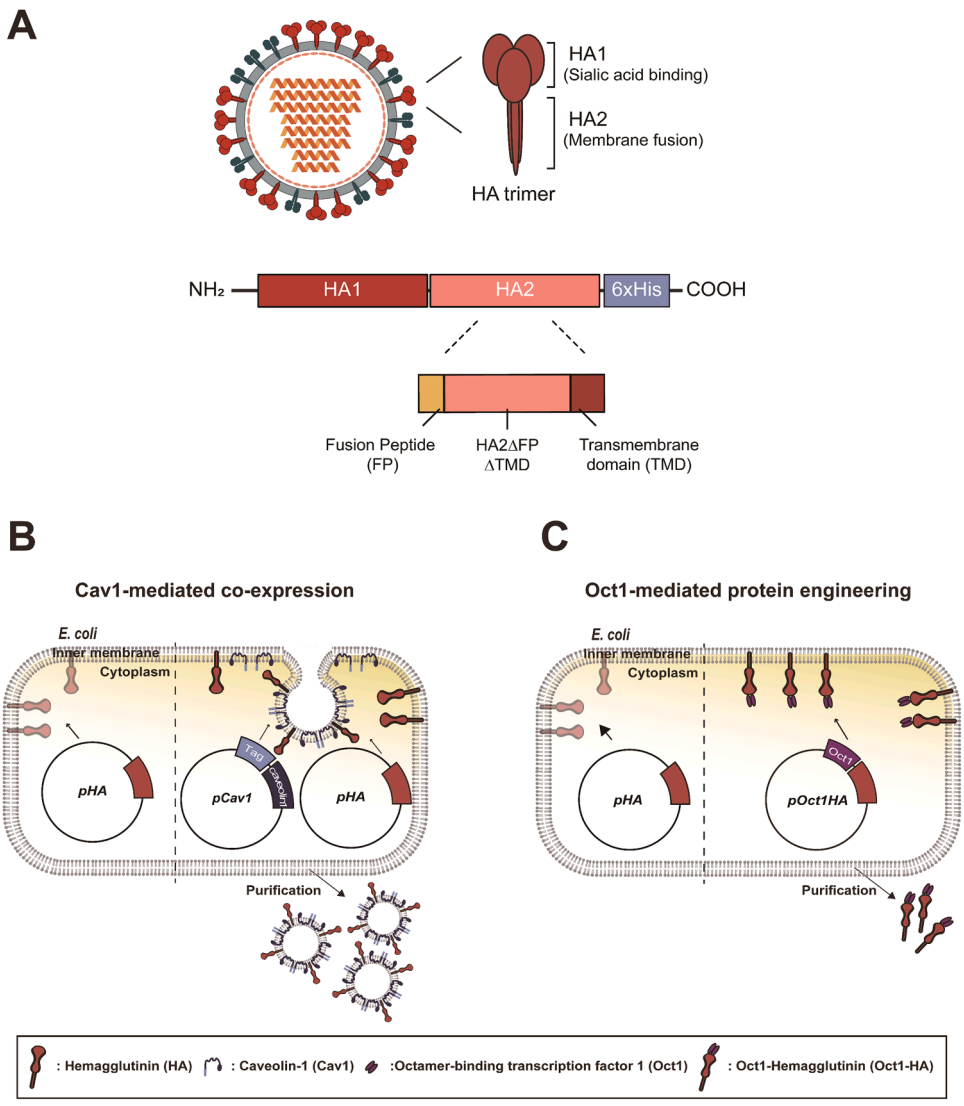

Fig. 1. Structural characteristics of hemagglutinin (HA) and schematic design of HA expression.

Table 1
List of strains and plasmids used in this study.

Strain/ plasmid	Relevant description	Antibiotic marker
E. coli TOP10	*F– mcrA Δ(mrr-hsdRMS-mcrBC) Φ80lacZΔM15 ΔlacX74 recA1 araD139 Δ(ara leu) 7697 galU galK rpsL (StrR) endA1 nupG*	-
E. coli BL21 (DE3)	*F – ompT hsdSB (rB- mB-) gal dcm* (DE3)	-
pHW2000-HA	pHW2000 + HA (A/hvPR8/34(H1N1)) (Genbank accession No: ABP64721)	
pHA2ΔFPΔT	pET28b + pTruncated HA(HA2 subunit (HA devoid of fusion peptide domain and transmembrane domain, HA2ΔFPΔT)	Active Ingredient
pHA2ΔFP	pET28b + pTruncated HA (HA2 subunit (HA devoid of fusion peptide domain, HA2ΔFP))	Active Ingredient
pHA	pET-28b + pHW2000-HA	Active Ingredient
pOct1-HA	pOct1-PS + pHA	Active Ingredient
p6xHis-Cav1	pACYC-Duet vector (Invitrogen) + caveolin 1 (Genbank accession number 403980)	Chloramphenicol
pMBP-TEV-Cav1	pMalC2X + pGST-Cav1 + TEV site	Chloramphenicol
pOct1-Cav1	pOct1-PS + pGST-Cav1	Chloramphenicol

cloning method: (1) Linearization of plasmid by PCR. (2) Preparation of insert with ≥ 15 base pair homology to the plasmid backbone by PCR. (3) Mix (1) with (2). (4) Treat T4 DNA polymerase at room temperature to generate 3′ overhangs. (5) Incubation on ice and perform transformation [16]. Insert or vector nucleotides were amplified using Pfusion Plus DNA Polymerase (Elpis Biotech, Daejeon, South Korea) or Phusion High-Fidelity DNA Polymerase (New England Biolabs, MA, USA) and digested with *Dpn*I. The insert nucleotides were phosphorylated at 37 °C for 30 min using T4 polynucleotide kinase (New England Biolabs, MA, USA) and ligated to the plasmid backbone using T4 DNA polymerase (New England Biolabs, MA, USA). The resulting plasmids were used to transform *E. coli* TOP10 hosts and subsequently sequenced.

2.2. Expression test

pHA was co-transformed with p6xHis-Cav1 or pMBP-TEV-Cav1, whereas pOct1-HA was co-transformed with p6xHis-Cav1, pMBP-TEV-Cav1, or pOct1-Cav1. Recombinant *E. coli* BL21 (DE3) strains were cultured in 25 mL of TB (Terrific Broth) containing antibiotics at 37 °C and agitation at 180 rpm. When OD_{600} reached 1.0, protein expression was induced at 25 °C for 6 h by adding isopropyl b-D-1-thiogalactopyranoside to a final concentration of 1 mM. The induced cultures were harvested and disrupted using a high-pressure homogenizer

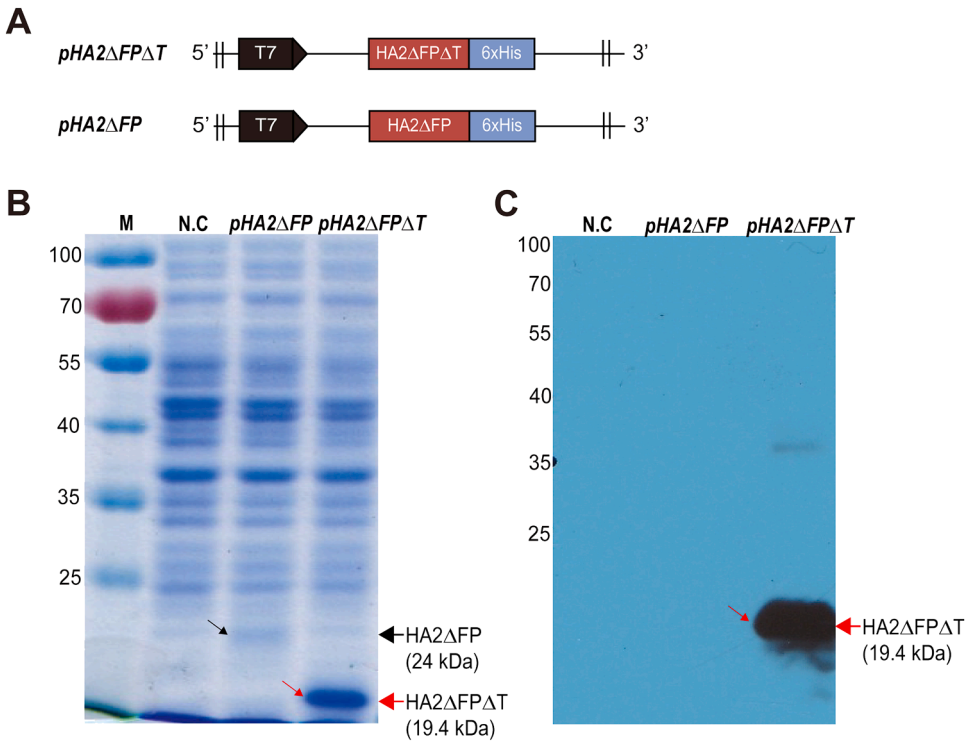

Fig. 2. Expression of truncated HA2 with or without TMD.

Nanogenizer (Genizer LLC, Irvine, CA, USA). Cell lysates were separated into soluble and insoluble fractions, which were then subjected to SDS-PAGE.

2.3. Western blot analysis

Purified proteins or cell lysates were separated on 10 % polyacrylamide gels. The loaded samples were prepared by mixing 6x sample buffer (50 mM Tris-HCl (pH6.8), 5 % beta-mercaptoethanol, 2 % sodium dodecyl sulfate, 10 % glycerol, 0.008 % bromophenol Blue). At this time, the insoluble pellet was sampled by dissolving it in the same amount of buffer as the soluble supernatant (40 mM Tris-HCl, pH 7.5, 300 mM NaCl, 5 mM imidazole, and 1 % % n-Dodecyl-beta-Maltoside (DDM)). The samples were heated at 100 °C for 10 min. The separated proteins were transferred to nitrocellulose membranes (GE Healthcare, IL, USA), blocked with 5 % skim milk in TBST buffer (50 mM Tris, pH 7.5, 150 mM NaCl, 0.05% Tween-20) for 1 h, and incubated with anti-Cav1 (Cell Signaling Technology, MA, USA) or anti-HA(Sino Biological Inc., Beijing, China), anti-His (Abcam, Cambridge, UK) antibodies at 1:5000 dilution for 16 h at 4 °C. The membranes were then washed with TBST buffer and incubated with anti-rabbit secondary antibodies (Sigma-Aldrich, MO, USA) at 1:20,000 and finally visualized by exposure to X-ray film (Agfa Health Care, Mortsel, Belgium).

2.4. Protein purification

Recombinant *E. coli* BL21 (DE3) was cultured in TB supplemented with 50 mg/mL Active Ingredient under the conditions of 37 °C and 180 rpm shaking speed. Thirty-four milligram per milliliter of chloramphenicol was added to the suspensions that were co-transformed with the Cav1 expression vector. When the OD_{600} of the culture reached 0.5, 1 mM IPTG was added, and protein was expressed at 25 °C for 6 h. Cells were collected by centrifugation at 8000 rpm for 5 min. Each inoculum was induced and collected in resuspension buffer (40 mM Tris-HCl, pH 7.5, 300 mM NaCl, 5 mM imidazole, and 1 % DDM) [17] at OD_{600} = 7 for sonication. After centrifugation at 12,000 rpm for 30 min, the soluble fraction of the cell lysate was loaded onto Ni-NTA beads (Bio-works, Uppsala, Sweden). The beads were washed with washing buffer (40 mM Tris-HCl, pH 7.5, 300 mM NaCl, 15 mM imidazole, and 0.1 % DDM). The protein of interest was eluted with elution buffer (40 mM Tris-HCl, pH 7.5, 300 mM NaCl, 500 mM imidazole, and 0.1 % DDM).

2.5. Immunization and HI assay

To obtain polyclonal antibodies against influenza A virus, 6-week-old female BALB/c mice were immunized by intramuscular injection. For comparison of the immunogenicity of Oct1-HA, a group of five mice were immunized with 4 μg Oct1-HA, and a group of five untreated mice were prepared as control. The Oct1-HA treated group was injected on day 0and boosted with an identical dose on day 14. On day 28, blood samples were collected from the mice via cardiac puncture and clotted for 1 h at 25 °C to isolate serum samples. Nonspecific inhibitors in the serum were inactivated by treating receptor destroying enzyme (RDE; Denka Seiken) prior to testing. Sera sample and RDE were mixed in a 1:3 ratio and incubated for more than 18 h at 37 °C. Then, the RDE reaction was terminated by heating at 56 °C for 30–60 min. The serum activity was tested in untreated 96-well cell culture plate, U type (SPL). RDE-treated serum was serially diluted by two-fold in the plate starting with a 10-fold initial dilution. An equal volume of virus (of each of two strains, A/hvPR8/34(H1N1) or A/X-31(H3N2)), adjusted to approximately 8 HA units/25 mL, was added to each well. PBS was used as a positive control instead of a virus. Non-immunized serum was used as a negative control. The plate was covered and incubated at 25 °C for 20 min followed by addition of 1 % (v/v) cRBCs (Innovative Research) in PBS and mixed by agitation. The plate was covered, and the cRBCs were allowed to settle for 30 min at 25 °C. The hemagglutination inhibition (HI) titer was determined by reciprocal dilution of the last well that contained non-agglutinated cRBCs. All animal experiments complied with the policies of the Institutional Animal Care and Use Committee of Sungkyunkwan University (IACUC number: SKKUIACUC2021-01-03-1).

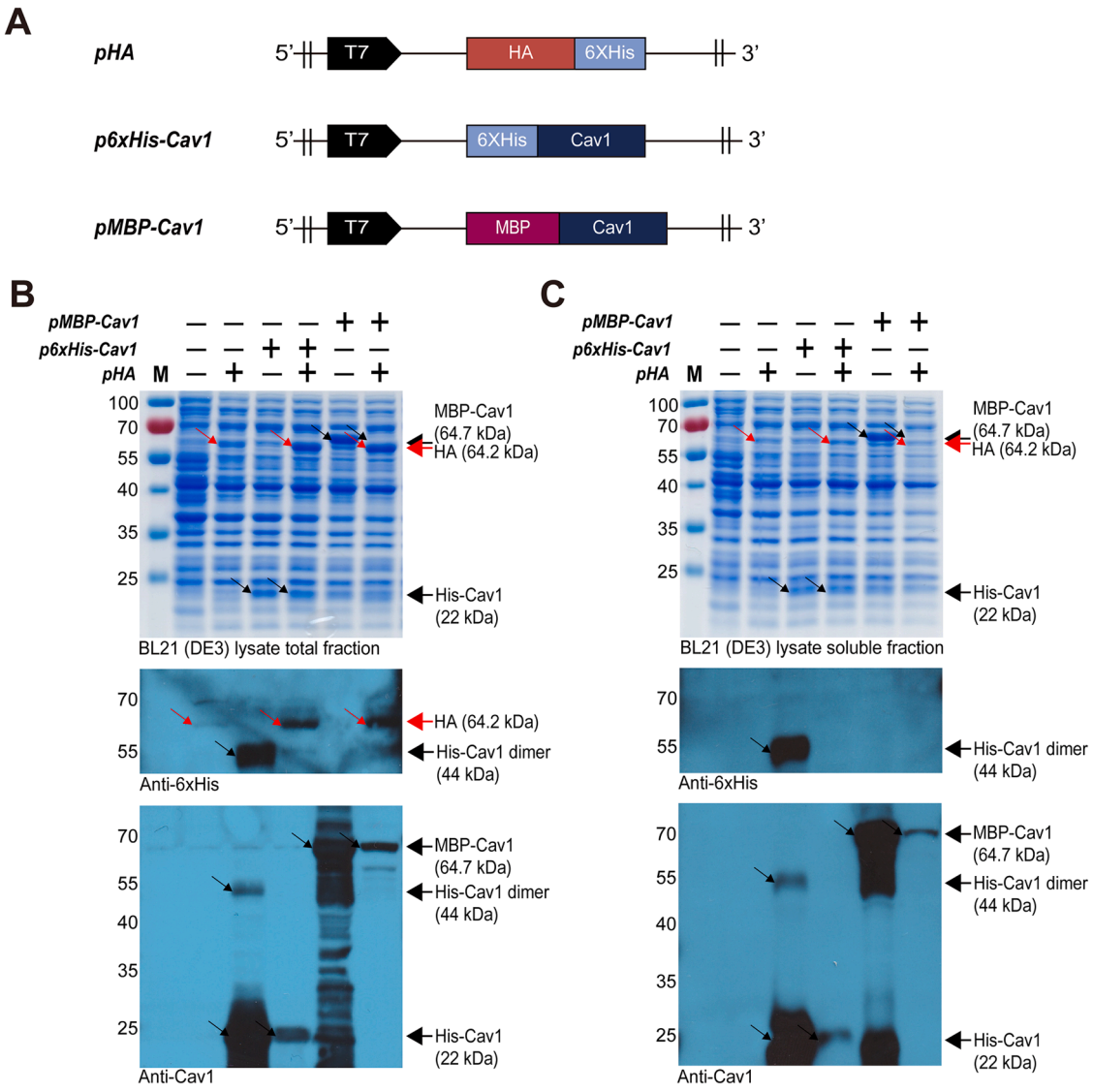

Fig. 3. Effect of Cav1 co-expression on full-length HA expression.

3. Results

3.1. Expression of HA2 lacking host fusion peptide

To investigate the influence of highly hydrophobic transmembrane domains (TMD) on the subunit HA2 expression, two plasmids carrying truncated HA2, lacking a fusion peptide (FP) domain, with or without TMD (pHA2ΔFP or pHA2ΔFPΔT, respectively) were constructed (Fig. 2A). SDS-PAGE showed that the truncated proteins migrated to their expected molecular weights: HA2ΔFP to 24 kDa; HA2ΔFPΔT to 19.4 kDa (Fig. 2B). In contrast to HA2ΔFPΔT, the expression of HA2ΔFP was low, as confirmed by western blot analysis (Fig. 2C). The extremely low expression level of TMD-harboring HA2 in *E. coli* led us to employ Cav1 co-expression and Oct1-fusion.

3.2. Synergistic aspect of Cav1 co-expression

Next, we examined the expression of full-length HA, with or without co-expression of heterologous Cav1 (Fig. 3). *E. coli* hosts were co-transformed with pHA and p6xHis-Cav1 or pMBP-TEV-Cav1, which were maintained using different antibiotic markers and origins of replication [18]. Two different tags (6xHis or maltose-binding protein, MBP) were tested for Cav1 and HA expression (Fig. 3A). We sought to identify whether 6xHis-Cav1 and MBP-Cav1 were expressed individually, and whether their expression affected the expression of HA. In the total cell lysate fraction, the band intensity of full-length HA (64.2 kDa) increased in the presence of both types of Cav1 (Fig. 3B). This was further confirmed in the blot image where individually expressed full-length HA was not detected, while comparable amounts of HA were identified in hosts co-expressing both types of Cav1 (Fig. 3B). However, such an expression change was not observed in the soluble fraction (Fig. 3C), and no HA expressed with or without Cav1 was detected by western blotting (Fig. 3C). This indicated that h-caveolae, which has been shown to form in *E. coli* cytoplasm upon Cav1 co-expression [5,9], could not be formed well when full-length HA was displayed on them while providing more membrane surface area to host the transmembrane protein. In conclusion, co-expression of Cav1 enhanced expression level of full-length HA.

3.3. Improved HA solubility associated with Oct1 fusion

To improve HA solubility, we introduced a fusion partner, the Oct1 DBD, with HA (pOct1-HA) or Cav1 (pOct1-Cav1) (Fig. 4A). Differences in Oct1-HA solubility was examined individually or together with h-caveolae tagged with various peptides (6xHis, 6xHis-Cav1; MBP, MBP-Cav1; Oct1-DBD, Oct1-Cav1) to determine any synergistic effect

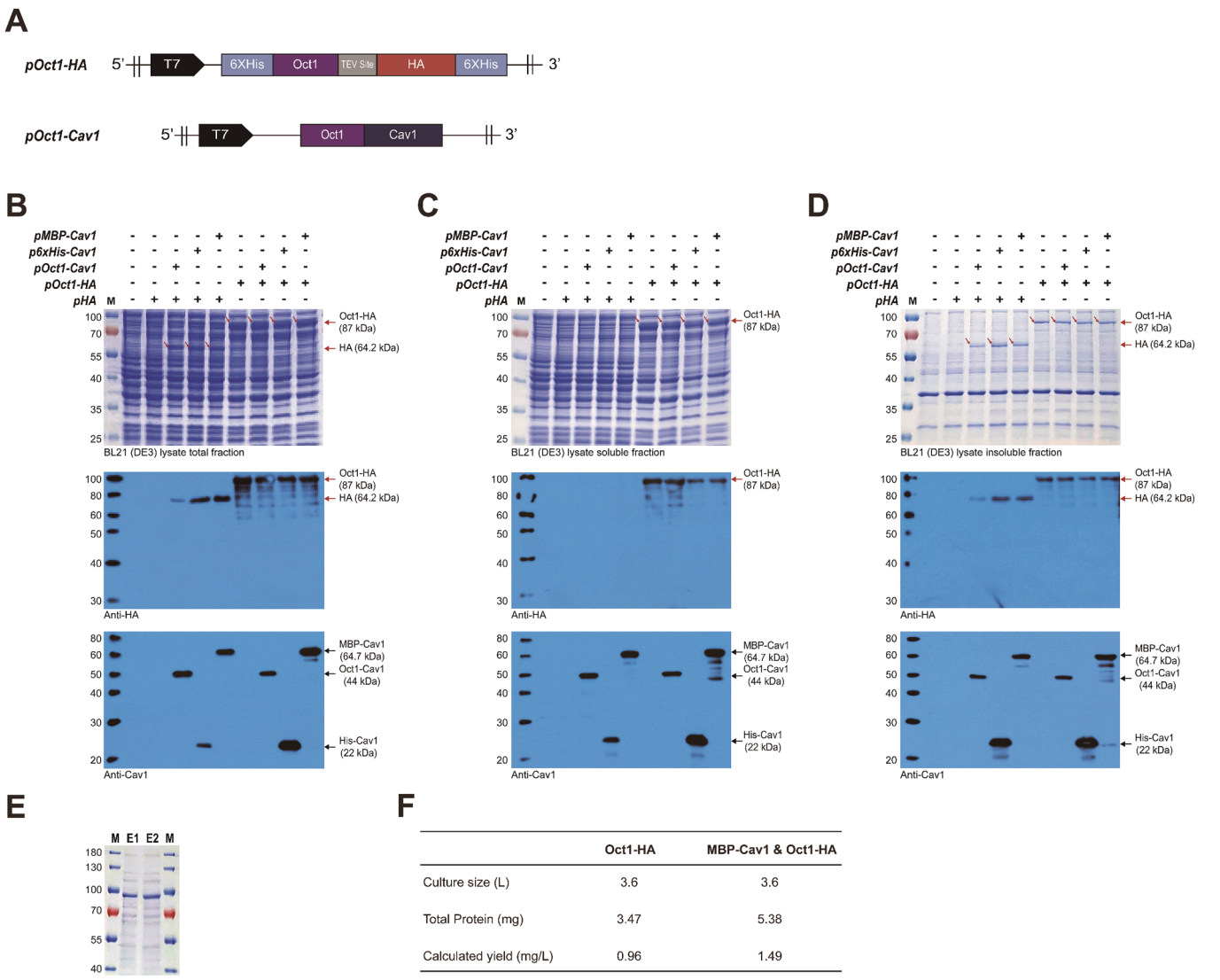

	Oct1-HA	MBP-Cav1 & Oct1-HA
Culture size (L)	3.6	3.6
Total Protein (mg)	3.47	5.38
Calculated yield (mg/L)	0.96	1.49

Fig. 4. Effect of Oct1 conjugation on the expression and purification of HA with or without co-expression of Cav1.

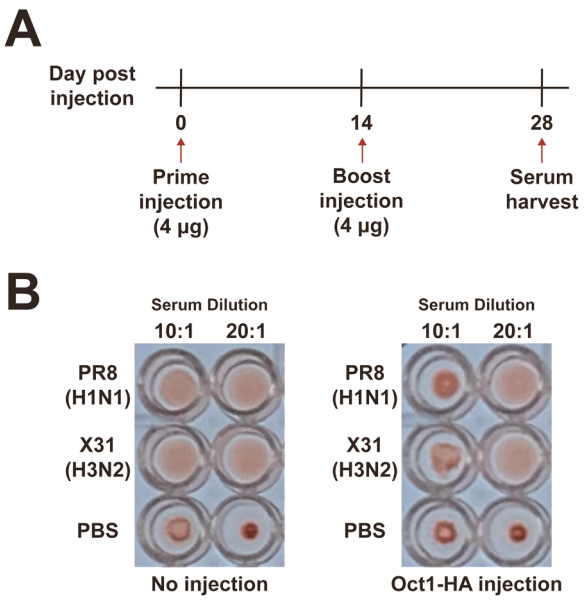

Fig. 5. Hemagglutination assay for determining activity of Oct1-HA.

(Fig. 4B, C, and D). The expression of HA alone and HA with expression partner was used as a control. According to the gel and western blot data, Oct1-HA (87 kDa) was detected in all the total cell lysates, regardless of Cav1 co-expression (Fig. 4B). Likewise, the presence of Oct1-HA was confirmed in the soluble fraction (Fig. 4C), whereas it was also present in the insoluble fraction (Fig. 4D). In contrast, the amount of HA co-expressed with MBP-Cav1 or 6xHis-Cav1 was low and was not identified in the soluble fraction. To better understand the effect of Oct1 fusion with or without Cav1 co-expression, the yield of total protein was calculated (Fig. 4F). As the yield increased by nearly 55 %, it is concluded that full-length HA expression benefits from Oct1-fusion and it can be further improved by Cav1 co-expression.

3.4. Activity of expressed Oct1-HA

To confirm the activity of Oct1-HA, an immune response was induced in mice using the expressed protein as an antigen. Two groups of 5 mice were set up. One group was a control group which was not injected with Oct1-HA, and the other group was injected with Oct1-HA. The mice were administered with or without antigen by intramuscular injection on day 0 and day 14 after Oct1-HA injection. On day 28, blood was collected via cardiac puncture, and serum was isolated (Fig. 5A). HI assay (hemagglutination inhibition assay) was conducted to verify

whether the Oct1-HA induced protective antibodies against two different subtypes of virus, PR8 (H1N1) and X31 (H3N2). No HI activity was observed without antigen injection. In contrast, both PR8 and X31 showed HI activity when Oct1-HA was injected (Fig. 5B). These results suggested that the expressed full-length HA was active.

4. Discussion

Hemagglutinin (HA) is key a factor in influenza vaccine development as (1) it is the most abundant protein on the viral surface, and (2) it can trigger immune responses. Among the subunits of HA, the HA2 stem region is more conserved in sequence than the HA1 subunit, and is less sensitive to the selective pressure of the immune system because it is occluded from the surface of influenza virions [19,20]. Accordingly, several attempts have been made to develop broad spectrum antibodies against the HA2 subunit, which comprises the stalk region of HA [21]. While expression of full-length or truncated HA2 subunits has been confirmed in bacterial systems, the protein products required additional re-folding and retained their activity and stability in detergents [22,23]. Regarding the soluble nature of the ectodomain between the FP and TMD [24], we expected that the removal of the FP would increase the feasibility of expression, thereby emphasizing the effect of the TMD. Compared to HA2ΔFPΔT, the expression of HA2ΔFP was hardly distinguishable (Fig. 2B and C), implying that the expression of truncated HA2 was significantly hindered by the presence of hydrophobic TMD. Considering the immunosubdominance of the stalk domain [25], we decided to focus on soluble expression and purification of full-length HA rather than on the truncated HA2 subunit.

Due to its ability to facilitate the overexpression of co-expressed transmembrane proteins via h-caveolae formation [5], Cav1 was expected to play a supportive role in the expression of full-length unmodified HA. Furthermore, it was assumed that co-expression of Cav1 and HA may result in the spontaneous formation of HA-embedded h-caveolae [5]. HA was identified in the total cell lysates of hosts co-expressing both types of Cav1, indicating an adjuvant effect (Fig. 3B), even though confirming the actual formation of HA-harboring h-caveolae by immunoblot assay was not possible due to the denaturation of vesicle structures in the reducing environment. However, increased HA expression was confirmed by higher band intensity in both the gel and blot images (Fig. 3B). Interestingly, both the blot images of total cell lysates (Fig. 3B) and soluble fractions (Fig. 3C) indicated that the amount of 6xHis-Cav1 and MBP-Cav1 were greatly reduced when co-expressed with HA, implying that their expression could be interrupted. Moreover, the intensities of both Cav1 bands in the soluble fractions (Fig. 3C) appeared to be weaker than those in total cell lysates (Fig. 3B). The reduced amount of Cav1 in the soluble fractions could be due to the effect of highly insoluble HA on the solubility of Cav1 and h-caveolae (Fig. 3C). We can conclude that Cav1 co-expression is insufficient for the soluble production of full-length HA. Therefore, we decided to adopt a fusion partner protein.

Oct1 fusion has been shown to dramatically improve the solubility of unstable proteins through intracellular plasmid display of the fusion proteins [10]. Similarly, Oct1-HA was successfully expressed in Cav1 co-expressing hosts as well as those not expressing Cav1 (Fig. 4B and C). Although the majority of Oct1-HA in the total cell lysate fractions was not in a soluble state (Fig. 4D), when compared with unmodified HA, fusion with Oct1 significantly increased the solubility of HA regardless of Cav1. These data imply that the auxiliary role of fused Oct1-DBD is sufficient for the soluble expression of HA, as there were no significant differences among Oct1-HA expression levels observed for all four recombinant strains. Moreover, Oct1-HA maintained its solubility during affinity chromatographic purification (Fig. 4E), verifying the contribution of Oct1 to the overall stability of HA. Moreover, we could confirm the supportive role of MBP-Cav1 in the solubility of Oct1-HA during purification (Fig. 4F). Meanwhile, contrary to Fig. 3, there were no detectable differences in band intensity of 6xHis-Cav1 and MBP-Cav1, indicating that the amount of both Cav1 variants was maintained at comparable levels in total cell lysates and soluble fractions (Fig. 4B and C). Such observations implied that fusion with Oct1-DBD can significantly improve the expression and solubility of HA and facilitate the formation of soluble virus-like particles (VLPs). When caveolin was expressed in tandem with Oct1-HA, reconstituted h-caveolae were generated (data not shown). In addition, immunogenicity of Oct1-HA was confirmed by hemagglutination inhibition (Fig. 5). Thus, it can be suggested that Oct1 fusion and caveolin co-expression would greatly contribute to the utilization and delivery of HA by VLP formation, ultimately promoting the development of broadly active influenza vaccines.

Table 2
Strategy of this work.

Strategy	Results
1. Co-expression with Cav1	1. Expression of HA 2. Insoluble expression
2. Fusion with Oct1 DBD	1. Soluble expression of HA
3. Co-expression with Cav1 & Fusion with Oct1 DBD	1. Soluble expression of HA, 2. Higher production yield

In conclusion, the expression of full-length unmodified HA, including the highly hydrophobic TMD in *E. coli*, was achieved by caveolin co-expression, whereas no soluble HA was identified. Thus, Oct1-DBD was fused with HA, contributing to the expression and purification of the fusion protein in its soluble form. The approaches and corresponding results to express full-length HA are summarized in Table 2. To our knowledge, this is the first study to successfully acquire soluble HA from a bacterial expression system, and we expect the achievements of this research to be utilized for and contribute to the development of a universal influenza vaccine.

CRediT authorship contribution statement

JC, YB, WP and DK designed the experiments. YB and WP performed the experiments. JC and YB and WP analyzed the data. JC and YB and WP drafted the manuscript and DK completed the manuscript. All authors have read and approved the final manuscript.

Declaration of Competing Interest

The authors declare that they have no known competing financial interests or personal relationships that could have appeared to influence the work reported in this paper.

Data Availability

Data will be made available on request.

Acknowledgements

This study was supported by the Basic Science Research Program through the National Research Foundation of Korea (NRF), funded by the Ministry of Education (Grant nos. 2020R1A2C2101964 and 2017R1A6A1A03015642).

References

[1] G.L. Rosano, E.A. Ceccarelli, Recombinant protein expression in Escherichia coli: advances and challenges, Front. Microbiol. 5 (2014) 172, https://doi.org/10.3389/fmicb.2014.00172.
[2] M.M. Carrió, A. Villaverde, Construction and deconstruction of bacterial inclusion bodies, J. Biotechnol. 96 (2002) 3–12, https://doi.org/10.1016/S0168-1656(02)00032-9.
[3] S. Falak, M. Sajed, N. Rashid, Strategies to enhance soluble production of heterologous proteins in Escherichia coli, Biologia 77 (2022) 893–905, https://doi.org/10.1007/s11756-021-00994-5.

[4] K.A.R. Packiam, R.N. Ramanan, C.W. Ooi, L. Krishnaswamy, B.T. Tey, Stepwise optimization of recombinant protein production in Escherichia coli utilizing computational and experimental approaches, Appl. Microbiol. Biotechnol. 104 (2020) 3253–3266, https://doi.org/10.1007/s00253-020-10454-w.
[5] J. Shin, Y.-H. Jung, D.-H. Cho, M. Park, K.E. Lee, Y. Yang, C. Jeong, B.H. Sung, J.-H. Sohn, J.-B. Park, D.-H. Kweon, Display of membrane proteins on the heterologous caveolae carved by caveolin-1 in the Escherichia coli cytoplasm, Enzym. Microb. Technol. 79–80 (2015) 55–62, https://doi.org/10.1016/j.enzmictec.2015.06.018.
[6] N. Jamin, M. Garrigos, C. Jaxel, A. Frelet-Barrand, S. Orlowski, Ectopic neo-formed intracellular membranes in Escherichia coli: a response to membrane protein-induced stress involving membrane curvature and domains, Biomolecules 8 (2018), https://doi.org/10.3390/biom8030088.
[7] F. Baneyx, M. Mujacic, Recombinant protein folding and misfolding in Escherichia coli, Nat. Biotechnol. 22 (2004) 1399–1408, https://doi.org/10.1038/nbt1029.
[8] V. Sączyńska, Influenza virus hemagglutinin as a vaccine antigen produced in bacteria, Acta Biochim. Pol. 61 (2014) 561–572, https://doi.org/10.18388/abp.2014_1878.
[9] P.J. Walser, N. Ariotti, M. Howes, C. Ferguson, R. Webb, D. Schwudke, N. Leneva, K.J. Cho, L. Cooper, J. Rae, M. Floetenmeyer, V.M. Oorschot, U. Skoglund, K. Simons, J.F. Hancock, R.G. Parton, Constitutive formation of caveolae in a bacterium, Cell 150 (2012) 752–763, https://doi.org/10.1016/j.cell.2012.06.042.
[10] Y. Park, J. Shin, J. Yang, H. Kim, Y. Jung, H. Oh, Y. Kim, J. Hwang, M. Park, C. Ban, K.J. Jeong, S.-K. Kim, D.-H. Kweon, Plasmid display for stabilization of enzymes inside the cell to improve whole-cell biotransformation efficiency, Front. Bioeng. Biotechnol. 7 (2020) 444, https://doi.org/10.3389/fbioe.2019.00444.
[11] J.H. Park, H.W. Kwon, K.J. Jeong, Development of a plasmid display system with an Oct-1 DNA-binding domain suitable for in vitro screening of engineered proteins, J. Biosci. Bioeng. 116 (2013) 246–252, https://doi.org/10.1016/j.jbiosc.2013.02.005.
[12] M. Ptashne, How eukaryotic transcriptional activators work, Nature 335 (1988) 683–689, https://doi.org/10.1038/335683a0.
[13] J.H. Jang, K.Y. Choi, Whole cell biotransformation of 1-dodecanol by Escherichia coli by soluble expression of ADH enzyme from Yarrowia lipolytica, Biotechnol. Bioprocess Eng. 26 (2021) 247–255, https://doi.org/10.1007/s12257-020-0176-5.
[14] H.-M. Lee, J. Ren, W.Y. Kim, P.N.L. Vo, S.-i. Eyun, D. Na, Introduction of an AU-rich element into the 5′UTR of mRNAs enhances protein expression in Escherichia coli by S1 protein and Hfq protein, Biotechnol. Bioprocess Eng. 26 (2021) 749–757, https://doi.org/10.1007/s12257-020-0348-3.
[15] Y.H. Lee, J.Y. Park, E.S. Song, H. Lee, M.U. Kuk, J. Joo, H. Roh, J.T. Park, Improvement of sleeping beauty transposon system enabling efficient and stable protein production, Biotechnol. Bioprocess Eng. 27 (2022) 353–360, https://doi.org/10.1007/s12257-021-0231-x.
[16] J.Y. Jeong, H.S. Yim, J.Y. Ryu, H.S. Lee, J.H. Lee, D.S. Seen, S.G. Kang, One-step sequence- and ligation-independent cloning as a rapid and versatile cloning method for functional genomics studies, Appl. Environ. Microbiol. 78 (2012) 5440–5443, https://doi.org/10.1128/aem.00844-12.
[17] D. Koley, A.J. Bard, Triton X-100 concentration effects on membrane permeability of a single HeLa cell by scanning electrochemical microscopy (SECM), Proc. Natl. Acad. Sci. USA, vol. 107, 2010, pp. 16783–7. ⟨https://doi.org/10.1073/pnas.1011614107⟩.
[18] N.H. Tolia, L. Joshua-Tor, Strategies for protein coexpression in Escherichia coli, Nat. Methods 3 (2006) 55–64, https://doi.org/10.1038/nmeth0106-55.
[19] E. Kirkpatrick, X. Qiu, P.C. Wilson, J. Bahl, F. Krammer, The influenza virus hemagglutinin head evolves faster than the stalk domain, Sci. Rep. 8 (2018) 10432, https://doi.org/10.1038/s41598-018-28706-1.
[20] A.M. Hashem, Prospects of HA-based universal influenza vaccine, BioMed Res. Int. 2015 (2015), 414637, https://doi.org/10.1155/2015/414637.
[21] B.L. Bullard, E.A. Weaver, Strategies targeting hemagglutinin as a universal influenza vaccine, Vaccines 9 (2021) 257, https://doi.org/10.3390/vaccines9030257.
[22] P.U. Ratnayake, E.A. Prabodha Ekanayaka, S.S. Komanduru, D.P. Weliky, Full-length trimeric influenza virus hemagglutinin II membrane fusion protein and shorter constructs lacking the fusion peptide or transmembrane domain: hyperthermostability of the full-length protein and the soluble ectodomain and fusion peptide make significant contributions to fusion of membrane vesicles, Protein Expr. Purif. 117 (2016) 6–16, https://doi.org/10.1016/j.pep.2015.08.021.
[23] A. Ranaweera, P.U. Ratnayake, D.P. Weliky, The stabilities of the soluble ectodomain and fusion peptide hairpins of the influenza virus hemagglutinin subunit II protein are positively correlated with membrane fusion, Biochemistry 57 (2018) 5480–5493, https://doi.org/10.1021/acs.biochem.8b00764.
[24] R.W. Ruigrok, N.G. Wrigley, L.J. Calder, S. Cusack, S.A. Wharton, E.B. Brown, J. J. Skehel, Electron microscopy of the low pH structure of influenza virus haemagglutinin, EMBO J. 5 (1986) 41–49, https://doi.org/10.1002/j.1460-2075.1986.tb04175.x.
[25] F. Krammer, P. Palese, Influenza virus hemagglutinin stalk-based antibodies and vaccines, Curr. Opin. Virol. 3 (2013) 521–530, https://doi.org/10.1016/j.coviro.2013.07.007.